Applied Catalysis B: Environmental 130–131 (2013) 257–263

Contents lists available at SciVerse ScienceDirect

Applied Catalysis B: Environmental

journal homepage: www.elsevier.com/locate/apcatb

Highly stable and efficient Ag/AgCl core–shell sphere: Controllable synthesis, characterization, and photocatalytic application

Bowen Ma, Jianfeng Guo, Wei-Lin Dai*, Kangnian Fan

Department of Chemistry and Shanghai Key Laboratory of Molecular Catalysis and Innovative Materials, Fudan University, Shanghai 200433, PR China

ARTICLE INFO

Article history:
Received 24 July 2012
Received in revised form 24 October 2012
Accepted 28 October 2012
Available online 22 November 2012

Keywords:
Ag/AgCl core–shell sphere
Photocatalysis
$FeCl_3$ oxidation
RhB degradation
Visible-light driven material

ABSTRACT

A new composite photocatalyst Ag/AgCl core–shell sphere was synthesized at room temperature by using a simple and generic approach. SEM images revealed that the as-prepared catalyst showed a uniform morphology with an average size of about 2 μm. The photocatalytic activity was significantly dependent on the molar ratio of Ag^0:Ag^+ on the surface of the catalyst, the optimum ratio being 0.035. Recycling experiments confirmed the excellent stability of the catalysts, without any silver leaching from the surface of the catalyst, suggesting that the photocatalyst Ag/AgCl core–shell sphere was a form of active and stable visible-light driven plasmonic material.

1. Introduction

Since the discovery of titanium dioxide's ability to split water under ultraviolet (UV) light, this semiconductor photocatalyst has been widely considered as a promising approach to solving environmental and energy problems [1,2,3,4,5,6,7,8,9]. However, the semiconductor materials available to date are generally limited by either poor photocatalytic efficiency in visible light region or by insufficient charge separation ability [10–13]. Therefore, in recent years much effort has been focused on the exploration and fabrication of novel materials as photocatalysts [14–21]. Among numerous novel photocatalysts, nanoparticles (NPs) of noble metals have recently attracted special attention because of their ability to strongly absorb visible light. These materials have been utilized to develop a plasmonic photocatalyst [16–21]. In particular, silver NPs formed on silver halide particles can show efficient photocatalytic activity in the visible region due to their plasmon resonance effect [18–27]. Recently, using an ion exchange and photoreduction method, Wang et al. [14,28] synthesized Ag@AgCl and Ag@AgBr plasmonic photocatalysts which showed excellent efficient photocatalytic activity under visible light irradiation. It is reported that silver halides, generally considered as photosensitive materials, can coexist stably with Ag NPs during the entire photocatalytic reaction process. Kakuta et al. [29] also observed that Ag^0 species could contribute to the smooth separation of electron–hole pairs on the $AgBr/SiO_2$ NPs and enable it to catalyze H_2 production from alcohol radicals. Later, a number of this kind of plasmonic photocatalysts were prepared and studied.

Among them, core–shell structured nanomaterials have attracted particular research attention in recent years because of their great potential in protection, modification, and functionalization of core particles, with suitable shell materials to enable specific physical, chemical, and biological performance [22–26]. Using in situ oxidation reaction, Bi and Ye [20] prepared Ag/AgCl core–shell nanowires which showed improved photocatalytic activity under visible light irradiation for the decomposition of methyl orange (MO) dye. Li et al. reported a feasible and effective solution route to synthesize Ag@AgCl coaxial core–shell nanocables via a controllable redox reaction between Ag nanowires [21]. Wang et al. synthesized AgBr nanoplates with exposed {1 1 1} facets in high yield by a facile precipitation reaction [27].

In spite of earlier research done on Ag-based core–shell nanoparticles [21–26], a comprehensive study on the photocatalytic activity and morphology-controlled synthesis is required to advance further applications owing to the fact that this series of photocatalysts has met some challenges, such as complicated synthesis process, need for recycling, stability and separation. We have attempted to find an approach to not only resolve the problems and disadvantages of this series of catalysts but also further improve their photocatalytic activity. In our previous work, we prepared super-paramagnetic core–shell $Fe_3O_4@SiO_2$ NPs through solvothermal and sol–gel method, and then fabricated $Ag–AgI/Fe_3O_4@SiO_2$ plasmonic photocatalyst via deposition–precipitation and photoreduction method [19]. In

* Corresponding author. Tel.: +86 21 55664678; fax: +86 21 55665572.
E-mail address: wldai@fudan.edu.cn (W.-L. Dai).

0926-3373/$ – see front matter © 2012 Elsevier B.V. All rights reserved.
http://dx.doi.org/10.1016/j.apcatb.2012.10.026

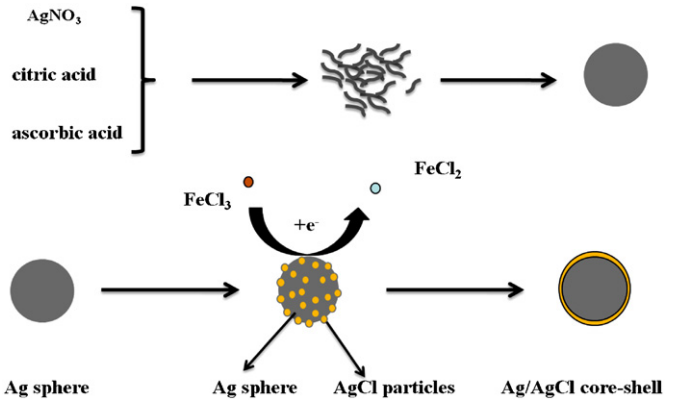

Scheme 1. Schematic description of the preparation of the core–shell Ag/AgCl sphere material.

addition, Ag/AgCl@cotton-fabric plasmonic photocatalyst has been synthesized by a facile method, which exhibits excellent stability for the decomposition of RhB and convenience in the separation and recovery of the catalyst from the solution [18].

In the present work, a feasible and effective approach has been reported for the first time to synthesize uniform Ag/AgCl core–shell spheres via a controllable oxidation reaction with different molar ratios of $FeCl_3$:Ag in solution at room temperature. The formation process of Ag/AgCl core–shell sphere was investigated in detail. Systematic investigations were also made on the influence of different molar ratios of the raw material on formation morphology, XRD diffraction peaks and optical absorption properties of Ag/AgCl core–shell sphere. Additionally, we studied the photocatalytic activity and stability of Ag/AgCl core–shell sphere; the optimal formation conditions were studied in relation to superior photodegradation of organic dyes. Much emphasis was directed at studying the correlation between photocatalytic activity and molar ratio of Ag^0:Ag^+ on the surface of the catalysts and the optimum ratio for best photocatalytic activity was attained.

2. Experimental

All chemicals were of analytical reagent grade and purchased from Sinopharm Chemical Reagent Co. Ltd. (SCRC), and used without further purification. The synthesis process is shown as Scheme 1.

2.1. Preparation of Ag spheres using ascorbic acid as the reducing agent

$AgNO_3$ aqueous solution and citric acid aqueous solution were added to 100 mL of deionized water in a 250 mL beaker with a magnetic stirrer in an ice-water bath. An ascorbic acid aqueous solution was then quickly injected into the vigorously stirred mixture. The added ascorbic acid was kept at equal molar ratio to that of silver ions. The solution became khaki-colored immediately, and a large quantity of Ag particles was produced in a few minutes. After 15 min, the particles were collected by centrifugation and repeatedly rinsed with deionized water. Ag spheres were obtained after the samples were dried at 60 °C for 5 h.

2.2. Preparation of Ag/AgCl core–shell sphere using ferric chloride

In a typical Ag/AgCl core–shell sphere synthesis, the reaction mixture containing the as-synthesized Ag spheres solution was added to an aqueous solution containing 50 mM PVP. Then, a certain amount of $FeCl_3$ (the molar ratio of Fe:Ag = 1:10, 1:5, 1:2, 1:3, 1:4, 1:1 and 2:1) was slowly added dropwise to this Ag spheres solution. The resulting mixture was maintained at room temperature until its color turned brown. Vigorous stirring was employed throughout the synthesis. The as-obtained samples for morphology and structure analysis were washed with water and ethanol to remove the $FeCl_3$ and PVP via centrifugation. Finally, pure Ag/AgCl core–shell spheres were obtained. It is known that the aqueous solution of $FeCl_3$ always contains HCl during the preparation process so that the reaction was carried out in an acidic media in which FeOOH or $Fe(OH)_2$ could not exist stably. As shown in Fig. S7, there is no Fe-containing compounds on the surface of the as-prepared catalysts.

2.3. Characterization

XRD patterns of the as-prepared samples (2θ ranges from 10° to 70°) were recorded at room temperature with scanning speed of 2° min^{-1} using Cu Kα radiation (λ = 0.154 nm) from a 40 kV X-ray source (Bruker D8 Advance). Diffuse reflectance spectroscopy was performed using a SHIMADZU UV-2450 instrument with a collection speed of 40 nm min^{-1} using $BaSO_4$ as the reference. Scanning electron micrographs (SEM) were obtained using a PHILIPS XL 30 microscope operating at accelerating voltage of 20 kV. X-ray photoelectron spectroscopy (XPS) measurements were performed on a PHI 5000 C ESCA System with Mg Kα source at 14.0 kV and 25 mA. All the binding energies were referenced to the contaminant C1s peak at 284.6 eV of the surface adventitious carbon.

2.4. Evaluation of photocatalytic activity

Photocatalytic experiments were performed in a beaker placed under a lamp bracket containing aqueous suspensions of rhodamin B (RhB) (100 mL, 50 mg L^{-1}), methyl orange (MO) (100 mL, 20 mg L^{-1}) and 50 mg of catalyst powder. The light source was a 125 W metal halide lamp (Philips) equipped with wavelength cut-off filters for λ ≤ 420 nm and focused on the beaker. Prior to the irradiation, the suspension was ultrasonicated for 10 min and then stirred in dark for 30 min to achieve the adsorption/desorption equilibrium. After turning on the lamp, 2 mL of suspension was sampled at certain time intervals (10 min) and centrifuged by centrifuge (Shanghai Anting Scientific Instrument Factory, China) at 13,000 rpm for 10 min to remove the particles. The upper clear liquid was analyzed by recording the characteristic absorption peak of RhB or MO at 550 nm or 463 nm to calculate the concentration of the compounds according to the standard work curve obtained previously.

3. Results and discussion

Fig. 1 displays the XRD patterns of the plasmon photocatalyst Ag/AgCl core–shell sphere synthesized by using different molar ratios of Fe:Ag (1:10, 1:5, 1:1 and 2:1). All the diffraction peaks can be indexed to cubic phase of Ag crystals (JCPDS file: 65-2871) and cubic phase of AgCl (JCPDS file: 31-1238) respectively, which confirms the formation of AgCl nanocrystals on the surface of the Ag spheres. The diffraction peaks are marked clearly in Fig. 1. As shown, with increase in molar ratio of $FeCl_3$:Ag, the characteristic peaks at 2θ of 38.1° and 44.4° indexed to the (1 1 1) and (2 0 0) planes of cubic Ag decreased gradually during the oxidation process while the characteristic peaks at 2θ of 32.2° and 46.2° corresponding to the (2 0 0) and (2 2 0) planes of cubic AgCl increased significantly. When the sample was prepared with the Fe:Ag molar ratio of 2:1, the (1 1 1) and (2 0 0) peaks of cubic Ag disappeared. Therefore, we assume that almost all Ag spheres were etched and transformed into AgCl crystals. Additionally, except for the metallic Ag and AgCl, no diffraction patterns corresponding to other impurity crystals

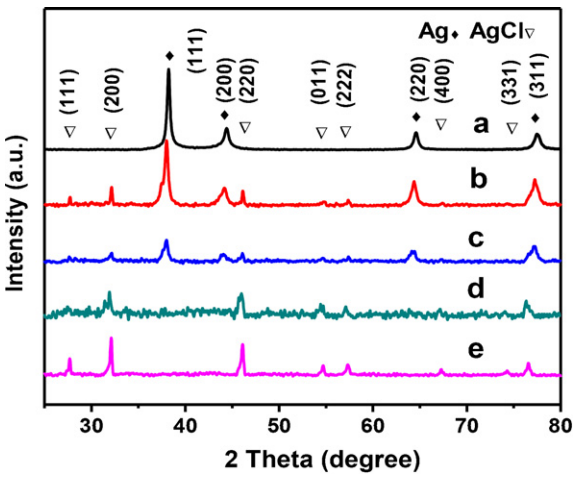

Fig. 1. Typical XRD patterns of Ag sphere (a), Ag/AgCl-1:10 (b), Ag/AgCl-1:5 (c), Ag/AgCl-1:1 (d) and Ag/AgCl-2:1 (e).

were observed, indicating that the obtained core–shell heterostructures in the whole growth process consisted only of metallic Ag and AgCl crystals; the thickness of AgCl nanoshells could be easily adjusted.

SEM images of the Ag spheres and the Ag/AgCl core–shell spheres are presented in Fig. 2. Images with low and high magnification are shown in A and B, respectively. It can be clearly seen that the as-prepared Ag spheres show a uniform shape with an average diameter of 1.0 μm. Addition of citric acid leads to the formation of perfect microspheres (1.0 μm in diameter) that are assembled by numerous closely packed Ag nanowires (Fig. 2B). As a result, the surface of the Ag spheres prepared is rough and beneficial to the oxidation reaction. Fig. 2C and D shows the SEM images of the Ag/AgCl core–shell spheres prepared by the Fe:Ag ratio of 1/1. It is interesting to find that after the oxidation, the morphology of the spheres was not changed noticeably. However, the diameter of the spheres increased to 2 μm, which is two times as large as that of silver spheres. Fig. 3J clearly shows that the core–shell spheres were actually formed by assembled nanosheets arranged along different directions, indicating that the surface of the catalysts had changed from silver to silver chloride. Fig. 2E shows the EDS spectrum of the Ag/AgCl core–shell spheres; it can be seen that silver and chlorine elements were present in the samples. Fig. 3 shows the SEM images of the Ag/AgCl core–shell spheres synthesized at various molar ratios of Fe:Ag (1:10, 1:5, 1:1 and 2:1). From this image, it is obvious that the morphology of the materials varies with the change in the molar ratio. When the ratio was 1:10, the surface of the spheres was formed by assembled nanosheets of approximately uniform size and shape, and the edges were distinct. Upon increasing the amount of $FeCl_3$, the nanosheets grew in size, and the surface of the Ag/AgCl core–shell spheres became increasingly smooth as the ratio was increased to 1:5. Upon further increasing the ratio to 1:1, the outer spheres appeared to be tightly wrapped by a layer of nanosheets which was obviously larger than that when the ratio was 1:5. This observation indicates that most silver on the surface may be completely etched and AgCl nanocrystals were formed on the outer spheres. However, the morphology of the sphere materials was destroyed and the uniform size of the spheres disappeared when the ratio was further increased to 2:1. This result demonstrates that the growth of AgCl nanocrystals on the surface of catalysts was sufficient and that there was no need to increase the ratio of Fe:Ag to 2:1. Therefore, during the synthesis process, the optimal ratio of Fe:Ag is 1:1, which is well in agreement with the photocatalytic activity result. Fig. 3I and J clearly shows the core–shell structure of the as-prepared Ag/AgCl spheres after the samples were ground in an agate mortar in the presence of ethanol. It is also very interesting to find that the Ag core was surrounded by AgCl shell, as shown in the highlighted area.

Fig. 4 shows the UV–vis DRS spectra of the Ag sphere and Ag/AgCl core–shell spheres synthesized at various molar ratio of Fe:Ag (1:10, 1:5, 1:1 and 2:1). These materials showed strong absorption in the UV region, a typical characteristic of silver. It is interesting to find that the silver sphere sample showed almost no absorption peak in the 400–750 nm region, owing presumably to the absence of surface plasmon resonance of Ag NPs. We assume that the silver particles made of the silver sphere are not in nanoscale, and are too large to produce the surface plasmon absorption. However, the series of Ag/AgCl core–shell sphere photocatalysts exhibited broad absorption in the visible light region of 400–750 nm, owing

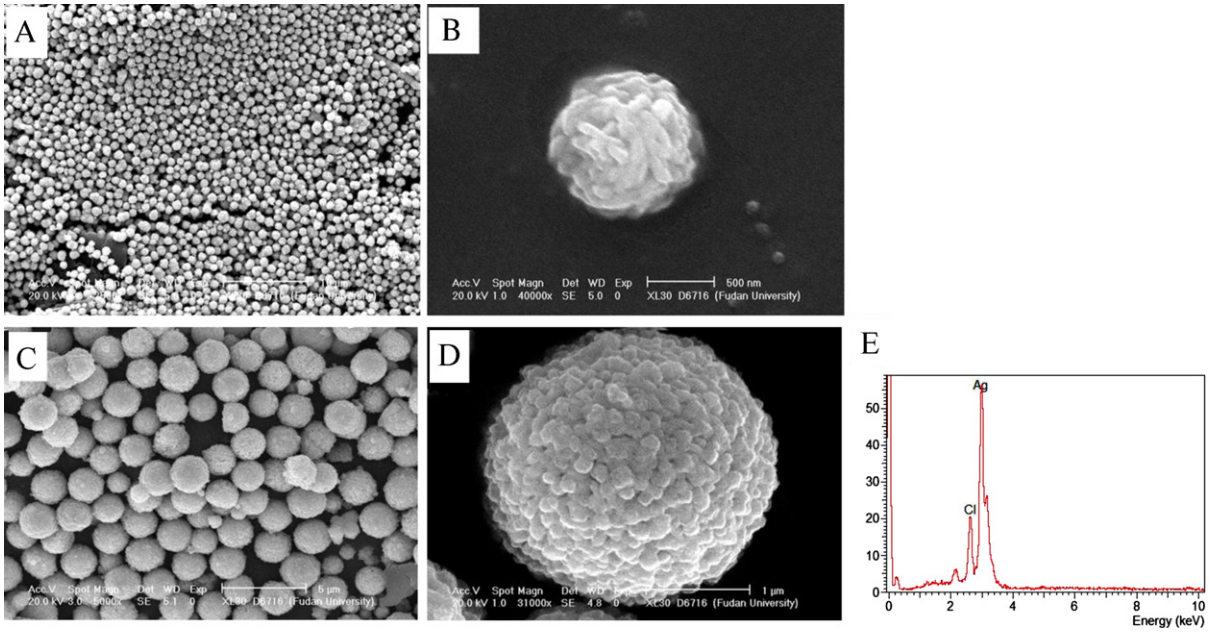

Fig. 2. Typical SEM images of the synthesized Ag sphere (A and B), Ag/AgCl core–shell sphere (C and D) and EDX of the Ag/AgCl core–shell sphere material (E).

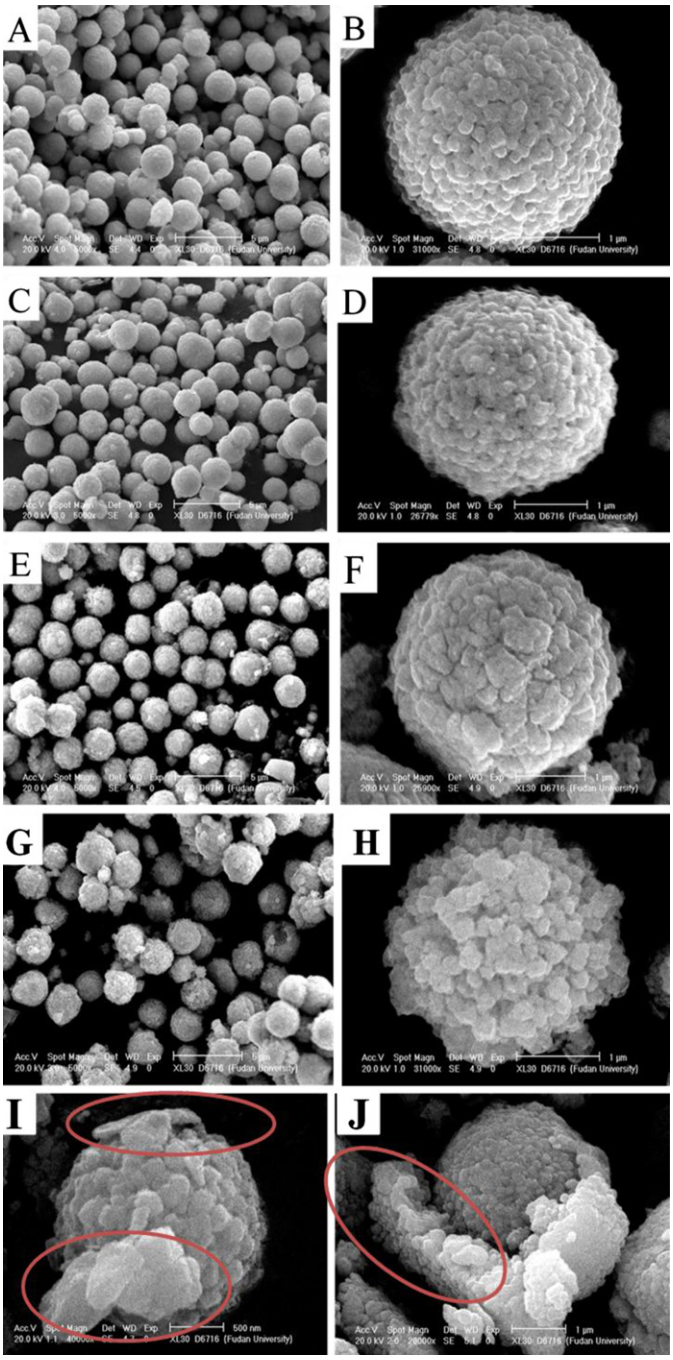

Fig. 3. Typical SEM images of Ag/AgCl-1:10 (A and B), Ag/AgCl-1:5 (C and D), and Ag/AgCl-1:1(E–J), Ag/AgCl-2:1 (G and H).

to the surface plasmon resonance of Ag NPs. During the oxidation reaction, the silver particles on the surface of spheres were etched by $FeCl_3$ and silver nanoparticles were formed. In accordance with the previous assumption, it was found that the absorption band at about 500 nm, due to the surface plasmon resonance of nano-sized silver, is proportional to the degree of oxidation. If more oxidant was used, the amount of Ag nanoparticles increased correspondingly while their size became progressively smaller. When the wavelength of the irradiating light was much larger than the diameter of silver NPs, the electromagnetic field across each entire silver NP was essentially uniform. With oscillations in the electromagnetic field, the weakly bound electrons of the silver nanoparticles respond collectively, giving rise to the plasmonic state. When the

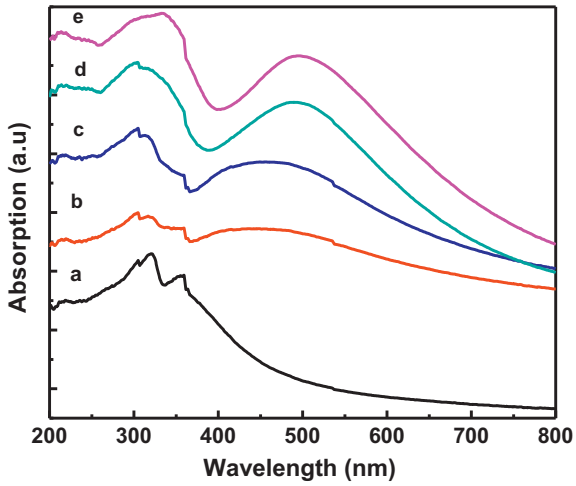

Fig. 4. Typical UV–vis DRS spectra of Ag sphere (a), Ag/AgCl-1:10 (b), Ag/AgCl-1:5 (c), Ag/AgCl-1:1 (d) and Ag/AgCl-2:1 (e).

incident light frequency matches the plasmonic oscillation frequency, the incident light is absorbed, resulting in surface plasmon absorption.

To evaluate the photocatalytic activity of series of Ag/AgCl core–shell spheres, the photodegradation of RhB and MO were carried out in aqueous dispersions under visible light irradiation. Fig. 5 shows the photocatalytic activity of the Ag/AgCl core–shell spheres prepared by using different molar ratio of Fe:Ag (1:10, 1:5, 1:2, 1:3, 1:4, 1:1 and 2:1). As shown, at irradiations of wavelengths of $\lambda > 420$ nm under visible light, the reaction showed limited photocatalytic activity for degradation of RhB in the absence of any catalysts; however, the presence of Ag/AgCl core–shell sphere catalysts resulted in very high photodegradation activity. Among the various Ag/AgCl core–shell spheres catalysts, the Fe:Ag (1:1) sample showed the most pronounced photocatalytic activity and could completely decompose RhB dye solution after irradiation for 20 min, similar to the reaction using Fe: Ag (2:1). Assuming that photodegradation of RhB dye follows a pseudo first order reaction mechanism, the degradation rate of RhB dye in the presence of different catalysts prepared with the molar ratio of Fe:Ag as 1:10, 1:5, 1:2, 1:3, 1:4, 1:1 and 2:1 were estimated to be 0.079, 0.097, 0.123, 0.124, 0.165, 0.246, and 0.246 mg min^{-1} respectively. This finding

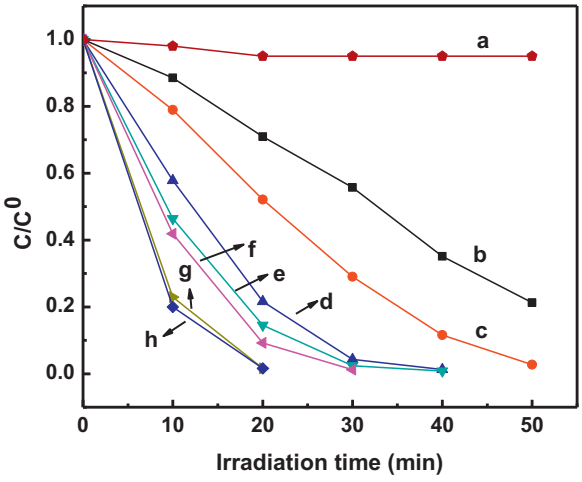

Fig. 5. Photocatalytic activities for the degradation of RhB dye under visible-light irradiation ($\lambda > 420$ nm) without catalyst (a) and over various Ag/AgCl core–shell spheres with different molar ratios of Fe:Ag (1:10 (b), 1:5 (c), 1:2 (d), 1:3 (e), 1:4 (f), 1:1 (g) and 2:1 (h)).

Table 1
Surface composition of Ag/AgCl core–shell sphere prepared by different molar ratios of Fe:Ag.

Sample	$FeCl_3$:$AgNO_3$ (M/M)	Ag^0/Ag^+[a] (M/M)	Ag/Cl[a] (M/M)
Ag/AgCl-1:10	1:10	2.31	2.10
Ag/AgCl-1:5	1:5	0.93	1.75
Ag/AgCl-1:2	1:2	0.79	1.12
Ag/AgCl-1:1	1:1	0.035	0.96
Ag/AgCl-2:1	2:1	≈0	0.63

[a] Molar ratio from XPS.

indicated that the photocatalytic activity of the samples was greatly enhanced by increasing of the molar ratio of ferric chloride to Ag, and subsequent oxidation from Ag spheres to AgCl crystal on the surface of the Ag spheres. According to previous reports [20,21], the photocatalytic activity is highly dependent on ratio of Ag:AgCl on the surface of the catalysts. There should be an optimum ratio for the best photoactivity. In a fair comparison of all the Ag/AgCl core–shell sphere samples, the Ag–AgCl sample prepared by a Fe:Ag (1:1) ratio may be considered as the best for optimum photoactivity. When the molar ratio was increased from 1:1 to 2:1, the photodegradation activity was not enhanced further. We believe that the oxidant was enough for the oxidation process when the molar ratio of Fe:Ag was 1:1. It should be noted that in aqueous dispersions under visible light irradiation, the photodegradation of MO (Fig. S1) shows similar trends to the RhB degradation, suggesting that the as-prepared core–shell spheres could serve as a general photocatalytic material. In addition, in order to eliminate the possibility of self degradation of dyes [30,31], we also evaluate the visible-light driven photocatalytic activity of the as-prepared catalysts on the degradation of p-chlorophenol. The result was shown in Fig. S8. It is interesting to find that after 30 minutes' reaction, p-chlorophenol was totally degraded, suggesting the superior photocatalytic performance of the Ag/AgCl core–shell spheres.

To further study the correlation between the ratio of Ag:AgCl on the surface of the catalysts and the photocatalytic activity, the surface composition of Ag/AgCl core–shell spheres was obtained from XPS measurements. As shown in Table 1, with increasing amount of ferric chloride, the ratio of Ag^0:Ag^+ decreased abruptly from 2.31 to approximately 0.0, while the Ag:Cl ratio decreased from 2.1 to 0.63. It is believed that with increasing amount of ferric chloride, more and more Ag atoms were oxidized to AgCl, which is in accordance with the results from the UV–vis DRS of the catalysts. In our previous work [18,32], it was concluded that the photocatalytic activity was highly dependent on the ratio of Ag:AgCl on the surface of the catalysts, and the best photocatalytic activity was elicited from the optimum ratio of Ag^0:Ag^+. Therefore the ratio of Ag:AgCl, obtained in the sample prepared by using Fe:Ag in (1:1) ratio, may be the best approach to achieve optimum photoactivity and the optimum ratio of Ag^0:Ag^+ was determined to be 0.035. This ratio appears to facilitate the interaction between Ag nanoparticles and AgCl crystals that results in the best photocatalytic activity.

To fully understand the photocatalytic activity and the interaction between Ag nanoparticles and AgCl crystals, a possible mechanism was proposed, as shown in Fig. 6, which is similar to that of Wang et al. [14]. According to this mechanism, during the degradation process, the oxidation reaction of H_2O takes place concurrently with the reduction of Ag^+, thus maintains stability in the whole system. Additionally, the reduction of Cl and re-oxidation of Cl^- happens during the photocatalytic reactions, therefore, the whole process serves as a photocatalytic reaction. Wang et al. [14] found that the surface plasmon resonance of Ag NPs, that results in an absorption in the 400–750 nm visible light region, may also prevent the recombination of photoexcited holes and electrons, and meanwhile lead to combination of Cl^- with the holes to form active Cl^0. The Ag NPs on the surface would play a key role on

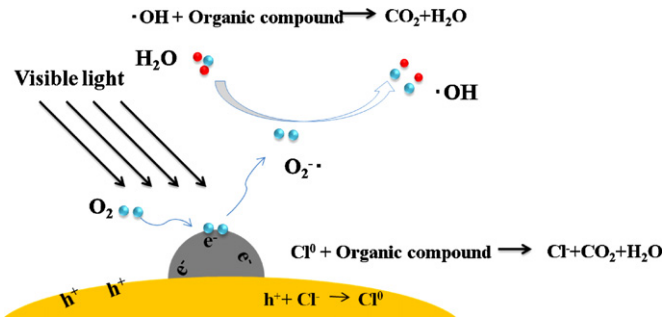

Fig. 6. Schematic diagram illustrating the photogeneration of electrons/holes as well as their migration and reaction in the surface of Ag/AgCl core–shell sphere.

the reaction. These Ag NPs would include some Ag NPs that come from the decomposition of AgCl shell, and some Ag NPs that were not oxidized. During the reaction, the surface of AgCl NPs becomes negatively charged because Ag^+ ions are reduced partially to Ag^0 species by visible light irradiation. The whole process of the degradation seems like a reaction cycle. In the present Ag/AgCl core–shell sphere system, when Ag/AgCl core–shell sphere in the solution was irradiated by the visible light, it is possible that electron–hole pairs are photogenerated in Ag NPs due to SPR effect. Then the photoexcited electrons can be transferred to the ubiquitous molecular oxygen to form the super-oxide radical O^{2-}, subsequently yielding the HOO• radicals through protonation; finally HO• radicals are also formed. All these active radicals can contribute to the decomposition of RhB. Simultaneously, the surface of AgCl NPs becomes negatively charged because Ag^+ ions are reduced partially to Ag^0 species by visible light irradiation, and the electric field of AgCl is likely terminated by Cl^- anions. Therefore, the photoexcited holes are transferred to the surface of AgCl NPs and cause the oxidation of Cl^- anions to Cl^0 atoms, which are subsequently able to oxidize RhB and to be reduced to Cl^- again. As a result, the Ag NPs can act as a sink for photodeduced charge carriers and be quickly renewed; the Ag/AgCl core–shell sphere photocatalytic system can stay stable due to the chloride reaction cycle. Further, if Ag NPs on the surface of the Ag/AgCl core–shell sphere are insufficient, the enhancement of photocatalytic activity by the surface plasmon resonance would be limited. If the Ag NPs were excessive, the energy levels may change to promote the recombination of the electrons and holes, which would reduce the photocatalytic activity of Ag/AgCl core–shell spheres. Additionally, if AgCl NPs were insufficient, the amount of Cl^0 radicals may be greatly reduced, which could also act as a factor in reducing the photocatalytic activity of samples. In conclusion, at the optimum ratio of 0.035, the interaction between Ag nanoparticles and AgCl leads to the best photocatalytic activity. This finding corroborates the mechanism proposed by Hu et al. [33].

For feasibility of use, the stability of a photocatalyst is as important as its photocatalytic activity. Therefore, the plasmon photocatalyst Ag/AgCl core–shell sphere was also investigated for stability through recycling experiments. As shown in Fig. 7A, the Ag/AgCl core–shell sphere sample did not show significant loss of photocatalytic activity even after three cycles of photodegradation of RhB dye. Fig. 7 shows that although photocatalytic activity decreased noticeably by fourth recycling, the sphere sample still maintained its spherical shape, indicating its excellent mechanical strength. The photocatalytic activity was completely recovered to its original value after the used spheres were oxidized with $FeCl_3$ again. During the second series of recycling tests, as shown in Fig. 7B, the sample did not show any significant loss of photocatalytic activity after three cycles of photodegradation of RhB. This result implies its promising potential for use in industry according to the following considerations: first, the deactivated spheres

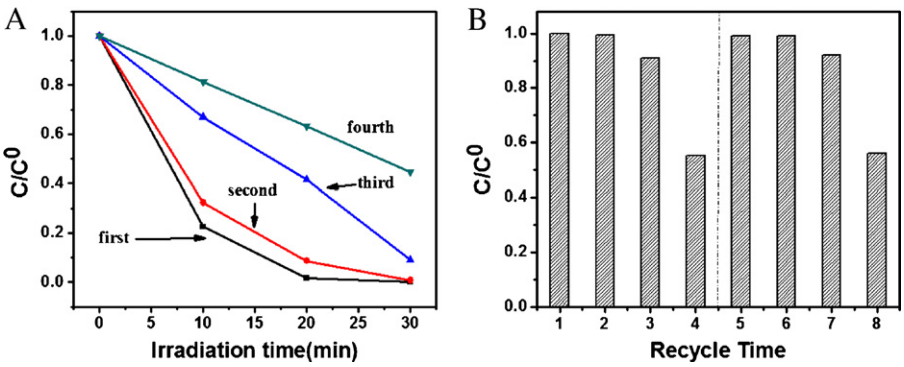

Fig. 7. Four consecutive cycling photodegradation curves of RhB dye over Ag/AgCl-1:1 core–shell sphere.

can be completely refreshed after treating with $FeCl_3$ solution at room temperature. The conditions required for this process are very mild and economic; second, no toxic, corrosive agents, or drastic conditions are required for the preparation and regeneration process of Ag/AgCl spheres, thus the synthetic process may be considered environmental-friendly; third, the Ag/AgCl core–shell sphere catalyst is very stable with excellent mechanical strength, and is recyclable for use as photocatalyst for several times; lastly, this material can be easily recovered and separated from the reaction mixture because of its special sphere shape and high density. Therefore, this material may be potentially used for photodegradation of hazardous pollutants in water under visible-light irradiation. In order to highlight the stability of the as-prepared photocatalysts, some contrastive experiments were carried out. The catalysts used in these experiments were refreshed and oxidized again after deactivation in the first use. Then the photodegradation of RhB solution was catalyzed by these refreshed catalysts. Fig. S9 shows the degradation ratio of RhB after 15 min reaction. It is apparent that the Ag/AgCl core–shell sphere catalyst shows excellent stability if compared with the previously reported Ag/AgCl/WO_3 one [32].

It is reasonable to expect that loss of active species on the surface of catalysts may seriously influence the photocatalytic activity when the catalysts are used repeatedly, leading to decrease in the stability of the materials. The existence of interior Ag core was beneficial for the stability and recycling of the as-prepared photocatalyst. It is known that the Ag/AgCl material always loses its active species such as AgCl nanoparticles and Ag NPs on the surface. The interaction between the Ag core and the surface active species in the present work would avoid this kind of activity loss. As shown in Fig. 8, solution in beaker A contained the catalyst after eight recycling runs while solution in beaker B contained 10 ppm silver nitrate solution. After being dripped with sodium chloride solution, A was still clear while B showed obvious white silver chloride precipitate. This simple test suggests that no silver ions had leached from the surface of the catalyst. All the above results indicate that the plasmon Ag/AgCl core–shell sphere is an active and stable visible-light driven plasmonic catalyst with a significant potential for practical use in the degradation of hazardous pollutants in water.

To further confirm the hypothesis on the use of oxidation process for synthesizing Ag/AgCl core–shell spheres, the morphologies of core–shell sphere products prepared with other halides were also investigated. As shown in Figs. S3 and S4, a comparison of the diameter of silver spheres, formed by using $CuBr_2$, showed that, the Ag/AgBr spheres had become two times larger after the oxidation, indicating that the outer silver had been etched and that AgBr shell was formed. Moreover, the EDS spectrum of the Ag/AgBr sphere showed that elemental silver and bromine were present in the samples. The XRD pattern suggests that these heterostructured products were composed of metallic Ag and AgBr crystals; no peaks from other materials were observed. Furthermore, when this oxidation process was performed in NaI and $Fe(NO_3)_3$ solution, the Ag spheres were also transformed into heterostructured products, as shown in Fig. S6. The photocatalytic activity of Ag/AgX (X = Br, I) core–shell spheres was also studied by carrying out the photodegradation of RhB in aqueous dispersions under visible light irradiation. Fig. S6 shows the photocatalytic activity of the as-prepared Ag/AgX (X = Br, I) core–shell spheres. It is clearly noted

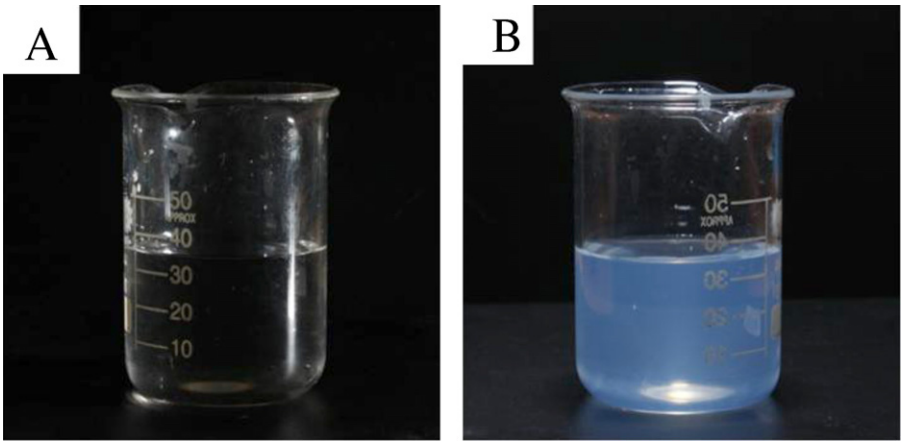

Fig. 8. Comparison images of the solution after 8 recycling experiment with Ag/AgCl spheres (A) and 10 ppm silver nitrate (B) after being dripped into sodium chloride solution.

that Ag/AgI showed excellent photocatalytic activity while Ag/AgBr exhibited unsatisfactory results. It is possible that silver bromide is more sensitive to irradiation of visible light, and degrades to silver rapidly, thus losing its photocatalytic activity.

4. Conclusions

In this work, the plasmonic photocatalyst Ag/AgCl core–shell sphere was successfully synthesized by a facile and effective method via an oxidation reaction between Ag spheres and $FeCl_3$ solution. The XRD analysis, SEM images and the UV–vis. DRS spectra all confirmed the formation of a core–shell structure. The ratio of Fe:Ag was found to influence the morphology and the photocatalytic activity of the as-obtained product; the optimal value of this ratio was found to be 1:1. It was also noted that the photocatalytic activity greatly depends on the ratio of Ag:AgCl on the surface of the catalysts; the optimum value of this ratio was found to be 0.035. The recycling experiments suggested that there was no leaching of silver from the surface of the catalyst.

All the above results indicate that the plasmon photocatalyst Ag/AgCl core–shell sphere is an active and stable visible-light-driven plasmonic catalyst, which serves as a promising candidate for practical use in the degradation of hazardous pollutants in water. The rational room-temperature synthetic strategy adopted in this study may be easily extended to fabricate other core–shell hetero-structures, leading to applications in several industrial fields such as electronics, sensing, photonics and separation.

Acknowledgements

This work was financially supported by the Major State Basic Resource Development Program (Grant No. 2012CB224804), NNSFC (Project 20973042, 21173052), the Research Fund for the Doctoral Program of Higher Education (20090071110011) and the Natural Science Foundation of Shanghai Science and Technology Committee (08DZ2270500).

Appendix A. Supplementary data

Supplementary data associated with this article can be found, in the online version, at http://dx.doi.org/10.1016/j.apcatb.2012.10.026.

References

[1] A. Fujishima, K. Honda, Nature 238 (1972) 37.
[2] B. O'Regan, M. Graetzel, Nature 353 (1991) 737.
[3] A. Fujishima, L.A. Nagahara, H. Yoshiki, K. Ajito, K. Hashimoto, Electrochimica Acta 39 (1994) 1229.
[4] P. Davis, D.L. Green, Environmental Science & Technology 33 (1999) 609.
[5] C. Hurum, K.A. Gray, T. Rajh, M.C. Thurnauer, Journal of Physical Chemistry B 109 (2005) 977.
[6] M.A. Fox, M.T. Dulay, Chemical Reviews 93 (1993) 341.
[7] J. Tang, Z. Zou, J. Ye, Angewandte Chemie International Edition 43 (2004) 4463.
[8] S. Wang, L. Yi, J. Halpert, X. Lai, Y. Liu, H. Cao, R. Yu, D. Wang, Y. Li, Small 8 (2012) 265.
[9] J. Du, X. Lai, N. Yang, J. Zhai, D. Kisailus, F. Su, D. Wang, L. Jiang, ACS Nano 5 (2011) 590.
[10] G. Tian, H. Fu, L. Jing, B. Xin, K. Pan, Journal of Physical Chemistry C 112 (2008) 3083.
[11] Y. Lai, M. Meng, Y. Yu, X. Wang, T. Ding, Applied Catalysis B: Environmental 105 (2011) 335.
[12] M. Hoffmann, S. Martin, W. Choi, D. Bahnemann, Chemical Reviews 95 (1995) 69.
[13] W. Yao, C. Huang, J. Ye, Chemistry of Materials 22 (2010) 1107.
[14] P. Wang, B. Huang, X. Qin, X. Zhang, Y. Dai, J. Wei, M. Whangbo, Angewandte Chemie International Edition 47 (2008) 7931.
[15] P. Wang, B. Huang, Z. Lou, X. Zhang, X. Qin, Y. Dai, Z. Zheng, X. Wang, Chemistry – A European Journal 16 (2010) 538.
[16] K. Awazu, M. Fujimaki, C. Rockstuhl, J. Tominaga, H. Murakami, Y. Ohki, N. Yoshida, T. Watanabe, Journal of the American Chemical Society 130 (2008) 1676.
[17] H. Li, Z. Bian, J. Zhu, Y. Huo, H. Li, Y. Lu, Journal of the American Chemical Society 129 (2007) 4538.
[18] B. Ma, J. Guo, W. Dai, K. Fan, Chinese Journal of Chemistry 29 (2011) 857.
[19] J. Guo, B. Ma, A. Yin, K. Fan, W. Dai, Applied Catalysis B: Environmental 101 (2011) 580.
[20] Y. Bi, J. Ye, Chemical Communications 43 (2009) 6551.
[21] F. Li, X. Liu, Y. Yuan, J. Wu, Z. Li, Crystal Research and Technology 45 (2010) 1189.
[22] A. Steinbru, A. Csaki, K. Ritter, M. Leich, J.M. Kohler, W. Fritzsche, Journal of Nanoparticle Research 11 (2009) 623.
[23] M. Abdulla-Al-Mamun, Y. Kusumoto, M.S. Islam, Chemistry Letters 38 (2009) 980.
[24] M.A. Lim, S.I. Seok, W.J. Chung, S.I. Hong, Optical Materials 31 (2008) 201.
[25] B. Sreedhar, P. Radhika, B. Neelima, N. Hebalkar, A.K. Mishra, Catalysis Communications 10 (2008) 39.
[26] O. Muehling, A. Seeboth, T. Haeusler, R. Ruhmann, E. Potechius, R. Vetter, Solar Energy Materials and Solar Cells 93 (2009) 1510.
[27] H. Wang, J. Gao, T. Guo, R. Wang, J. Li, Chemical Communications 48 (2012) 275.
[28] P. Wang, B. Huang, X. Zhang, X. Qin, H. Jin, Y. Dai, Z. Wang, J. Wei, J. Zhan, S. Wang, Chemistry – A European Journal 15 (2009) 1821.
[29] N. Kakuta, N. Goto, H. Ohkita, T. Mizushima, Journal of Physical Chemistry B103 (2009) 5917.
[30] X. Yan, T. Ohno, K. Nishilima, R. Abe, B. Ohtani, Chemical Physics Letters 429 (2006) 606.
[31] M. Mrowetz, W. Balcerski, A. Colussi, R. Hofmann, Journal of Physical Chemistry B108 (2004) 17269.
[32] B. Ma, J. Guo, W. Dai, K. Fan, Applied Catalysis B: Environmental 122–123 (2012) 193.
[33] C. Hu, T. Peng, X. Hu, Y. Nie, X. Zhou, J. Qu, H. He, Journal of the American Chemical Society 132 (2010) 857.